Mitt. Österr. Geol. Ges. | ISSN 0251-7493 | 89 (1996) | 201-212 | Wien, Dezember 1998

Schlüsselwörter
cooling curves
Koralpe
Gleinalpe
Swiss Alps
geothermometry

Distinguishing Cooling Histories using Thermometry. Interpretations of Cooling Curves with some Examples from the Glein-Koralm Region and the Central Swiss Alps.

KURT STÜWE AND KARIN EHLERS*)

7 Figures and 1 Table

Content

Dokumentation verschiedener Abkühlkurven mittels Geothermometrie. Zusammenfassung der Methodik und Anwendung auf die Interpretation von Abkühlkurven aus dem Glein-Koralm Bereich und den zentralen Schweizer Alpen.

Zusammenfassung

Kühlkurven von metamorphen Gesteinen sind in lineare, konkave und konvexe Kühlkurven unterteilbar. Bei linearen Kühlkurven bleibt die Kühlrate bei verschiedenen Temperaturen konstant. In konvexen Kühlkurven steigt die Kühlrate bei abfallenden Temperaturen an. Daß heißt, konvexe Kühlkurven sind in einem Diagramm nach oben *konvex*, wenn die Temperatur nach oben und die Zeit nach rechts aufgetragen wird. In konkaven Kühlkurven fällt die Kühlrate bei niederen Temperaturen ab, daß heißt sie sind nach oben *konkav*. Konkave Kühlkurven können zum Beispiel im Rahmen der Kontaktmetamorphose entstehen, wenn sich die Temperatur am Ende eines Erwärmungsprozesses asymptotisch an die ambiente Temperatur angleicht. Konvexe Kühlkurven können zum Beispiel entstehen, wenn Gesteine mit konstanter Geschwindigkeit exhumiert werden. Wir bezeichnen diese zwei Kühlprozesse als *passive* und *aktive* Kühlprozesse. Es wird allerdings betont, daß die Zuordnung zwischen Kühlprozeß und Form der Kühlkurve keineswegs eindeutig ist und stark von den geologischen Randbedingungen abhängt.

Der Formunterschied zwischen konkaven und konvexen Kühlkurven kann mit geothermometrischen Daten dokumentiert werden. Um dies zu zeigen koppeln wir einfache analytische Beschreibungen von konkaven und konvexen Kühlkurven mit der Formulierung für Schließtemperatur von DODSON (1973; 1986). Diese Formulierung stellt eine Beziehung zwischen Kühlrate, Korngröße und Diffusionskonstanten her und kann verwendet werden, um Zonierungsprofile in Mineralen zu interpretieren. Geothermometer, wie zum Beispiel das Granat-Biotit Thermometer, können daher dazu benutzt werden, um Kühlkurven zu dokumentieren und zwischen verschiedenen Kühlprozessen zu unterscheiden. Diese Information kann dazu verwendet werden, die unterliegenden tektonischen Prozesse zu interpretieren. Beispiele von der Eoalpinen Kühlgeschichte des Glein- und Koralm-Bereiches, der zentralen Schweizer Alpen im Bereich der Simplonlinie, sowie aus Schottland und Kanada, werden diskutiert. In den angeführten Beispielen wurde die Kühlkurve von anderen Autoren geochronologisch dokumentiert. Hier wird gezeigt, daß die Form der Kühlkurve auch mit geothermometrischen Daten belegt werden kann. Die Ergebnisse werden in Bezug auf die möglichen Kühlursachen diskutiert.

Abstract

The shape of cooling curves of metamorphic rocks is classified into curves of linear, convex and concave shape. Convex cooling histories are convex upwards in a diagram where temperature is plotted upwards and time towards the right. They have *increasing* cooling rates at low

*) Anschrift der Verfasser: Kurt STÜWE und Karin EHLERS, Institut für Geologie und Paläontologie, Universität Graz, Heinrichstraße 26, A-8010 Graz, Österreich. email of communicating author: kurt.stuewe@kfunigraz.ac.at.

temperatures. Concave cooling histories are concave upwards in a temperature-time diagram with *decreasing* cooling rates at low temperature. One of the causes of this difference in shape is the underlying cooling process. Concave cooling curves terminate by asymptotic equilibration to an ambient temperature; they may therefore be characteristic of cooling due to cessation of a heating process, for example contact metamorphism around intrusions. Convex cooling curves, on the other hand, are characterised by an increase in cooling rate at low T; for example because of the increasing effect of a cooling surface, as may occur during cooling due to exhumation. We term the two cooling processes *passive* and *active* cooling, respectively. However, we emphasize that the correlation of cooling process with the shape of cooling curve is ambiguous and depends strongly on the geological boundary conditions.

Simple expressions describing convex and concave cooling curves are used to demonstrate that the difference in shape of cooling curves may be extracted from the thermometric record of metamorphic rocks. Thus, geothermometric information may be used to distinguish between these two end member scenarios of cooling. This may provide important information on the tectonic environment. Examples of geochronologically established cooling histories from the Glein and Koralm region in the Eastern Alps, the central Swiss Alps, Scottland and Canada are used to predict their geothermometric record. The results are interpreted in terms of possible causes of cooling.

1. Introduction

The cooling history of metamorphic rocks bears important information on the tectonic environment of their formation. For example, advectively-heated terrains (like many low-P high-T terrains) are often considered to be characterised by rapid cooling (SANDIFORD et al., 1991), while conductively-heated terrains (like many Barrovian terrains) are often considered to cool slowly (ENGLAND & THOMPSON, 1984). In principle, such rate criteria are an appealing data set for constraining the geological processes that cause cooling. However, there is little understanding of absolute values for "fast" and "slow" cooling in geological environments and it is likely that there is overlap of cooling rates in different tectonic settings (e. g.: HODGES et al., 1994). It is therefore important to establish criteria of cooling histories that can be used to discriminate between different cooling processes. HARRISON & CLARKE (1979) showed that cooling curves following contact metamorphism have a different shape to those of cooling during exhumation. Many other cooling curves have since been documented using geochronology. Contrasting shapes have been observed in some examples (VANCE & O'NIONS, 1992). However, cooling curves documented with absolute ages and closure temperatures of different isotopic systems are always subject to potentially large uncertainties caused by a circular logic: prior to documenting a cooling curve, cooling curves have to be assumed to establish the closure temperatures of individual exchange systems. While the wide success of geochronologically-constrained cooling histories has shown that this circular logic does not appear to invalidate the results, it *is* desirable to find other methods to determine cooling curves by independent means.

Determining cooling curves from one exchange system is, in principle, possible since the work of DODSON (1973, 1986). DODSON (1973) demonstrated that, using different grain sizes, *one* exchange system can be used to determine a series of closure temperatures and this possibility has been suggested and used since (e. g.: MENGEL & RIVERS, 1991; EHLERS et al., 1994a, b). It is therefore possible to document substantial parts of a cooling curve from a single exchange system and the question arises: what is the information of an identified cooling curve on the underlying cooling process? In this paper we provide a simple parameterisation of different shapes of cooling curves as they may result from different cooling processes.

The purpose of this paper is therefore two-fold. Firstly, it is shown how cooling curves of different shape may relate to different cooling processes so that this parameterisation may be used to interpret a documented cooling curve. Secondly, it is discussed how thermometric information from *one* exchange system may be used to document the shape of a cooling curve. The discussion is then performed using a series of examples from the Alps and igneous intrusions in Scottland and Canada.

2. The model cooling histories

In parameterising cooling, three fundamentally different shapes of cooling curves are distinguished. These are: *linear*, *convex* and *concave* cooling curves in a temperature-time diagram. In convex cooling curves, cooling rates increase with time and decreasing temperature. That is, they are convex upwards in a diagram where temperature is plotted upwards and time towards the right and they have a negative slope in a temperature-cooling rate diagram (Figs. 1, 2). In concave cooling curves, cooling rates decrease with time and decreasing temperature. They are concave upwards in a temperature-time (T-t) diagram. They have a positive slope in a temperature-cooling rate diagram. In linear cooling curves the cooling rate remains constant with temperature. In parameterising these different shapes, we use simple descriptions of end member scenarios for cooling following contact metamorphism and cooling due to exhumation. The simple examples used have concave and convex cooling curves respectively and serve us here as an example for a simple geological process that cause a specifically-shaped cooling curve. We now discuss the model assumptions. The geological relevance of these simple end member models for cooling causes are discussed in the next section.

Convex cooling curves are described with a simple analytical model for cooling due to exhumation. This is described with the thermal history of a one-dimensional column with an initially linear thermal gradient g moving at a constant rate U through a surface of constant temperature. For these boundary conditions the heat flow equation may be solved analytically and the solution discussed in Appendix 2 will be used to quantify temperature-time paths (CARSLAW & JAEGER, 1959). Using (5) of Appendix 2, a large range of active cooling histories may be described by varying only two parameters: the thermal gradient g and the velocity U. These two variables are interpreted here as a geothermal gradient and the exhumation rate. With these assumptions, cooling rates at all depths increase continuously throughout the thermal evolution (Figs. 1, 2).

Concave cooling curves are here described with a simple analytical model for contact metamorphism around a cooling intrusion (JAEGER, 1964) (Appendix 2; Fig. 1a, inset). This model is a good description for cooling of magmatic bodies, but also for a range of other advective and productive heating processes (LUX et al., 1986; STÜWE et al., 1993; HOLM & DOKKA, 1993). The cooling rate, the maximum cooling rate and the peak temperature can be described as a function of time and distance from the intrusion with simple analytical expressions (Appendix 2). A wide range of cooling curves can be described by varying only two parameters: the intrusion diameter, d, and the distance of observation from the center of the intrusion, z, (Table 1, Appendix 1). Using this description, cooling curves begin with an increase in cooling rate following

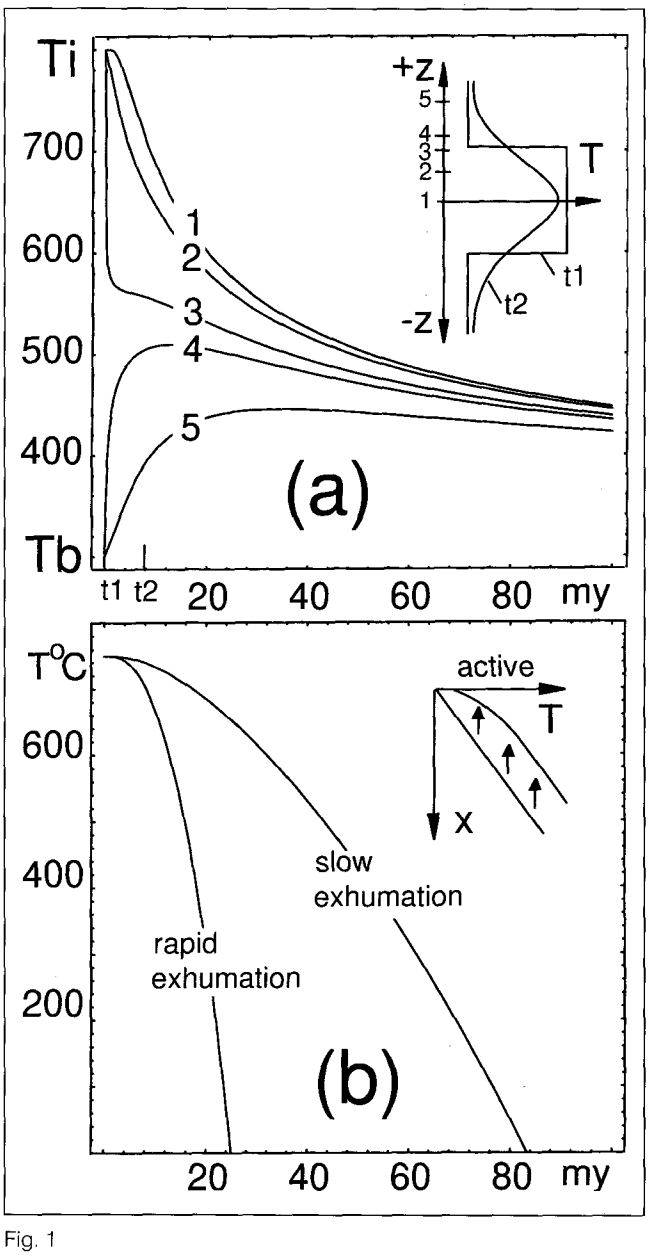

Fig. 1
A comparison of cooling curves during active and passive cooling as described by simple analytical expressions for end member scenarios of the two processes (Appendix 2). Fig. 1a shows passive cooling curves for five different locations with respect to a cooling intrusion illustrating that cooling curves are largely concave upwards in a *T-t* diagram. The distances corresponding to curves 1, 2, 3, 4 and 5 are z = 0, 15, 29, 35 and 50 km from the center of a d = 60 km thick intrusion, respectively. (1) has a cooling rate maximum after initial intrusion; in (2) the cooling rate maximum is at the metamorphic peak and decreases exponentially thereafter and (3) has two cooling rate maxima. At low temperatures, cooling rates for all curves decrease exponentially with temperature. Fig. 1b shows active cooling curves for two different exhumation rates of U = 300 m/my and 1000 m/my for g = 30 °C/km and x_i = 25 km. In contrast to Fig. 1a, cooling curves have no maximum cooling rate but increase continuously with proximity to the surface. The temperature-time curves are convex upwards in *T-t* space.

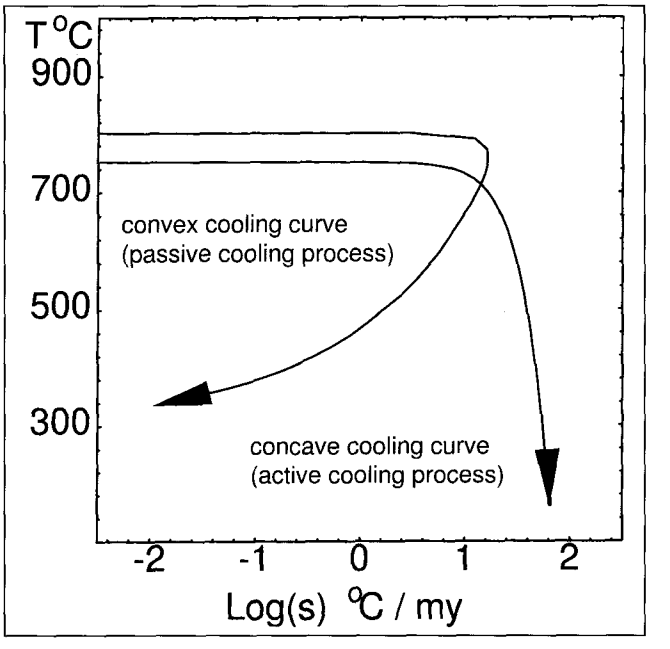

Fig. 2
A plot of cooling rate versus temperature illustrating the different shape of active and passive cooling curves. The example for active cooling corresponds to the cooling curve of rapid exhumation in Fig. 1b, the example for passive cooling corresponds to curve 1 in Fig. 1a. Both curves are calculated by direct differentiation of temperature with respect to time of the corresponding curves in Fig. 1a.

the contact metamorphic peak. This must occur as the metamorphic temperature peak is defined by no temperature change over time in the temperature-time cycle (Fig. 2). The shape of passive cooling curves also depends somewhat on the distance from the center of the intrusion. For example, material points near the contact at $z = d/2$ will have two cooling rate maxima (curve 3 on Fig. 1a), while all other distances have only one cooling rate maximum. Regardless, large parts of cooling curves for all z are concave upwards in a *T-t* diagram (Fig. 1).

The two end member examples discussed above will serve us as examples throughout the remainder of this paper. They illustrate that the geological processes causing cooling may have a profound influence on the shape of the cooling curve and it is intriguing to speculate that tectonothermal processes can be interpreted from the shape of cooling curves alone. In view of such speculations we will use the term *active cooling* for cooling processes that are caused by active transport of a rock towards a cooling surface. Active cooling processes will often cause *convex* cooling curves as the increasing effects of a cooling surface become stronger at lower temperatures when rocks get in closer proximity to the surface. We term *passive cooling* processes, processes in which cooling is caused by the termination of an earlier heating process, so that cooling is merely the consequence of thermal relaxation. This may be typical of cooling following contact metamorphism. Some geologically relevant parameter ranges for simple descriptions of active and passive cooling processes are discussed in Appendix 1. However, geologically realistic cooling processes are subject to a large variety of parameters influencing cooling. They include – among many others – the influence of topography (e. g. STÜWE et al., 1994) or the influence of episodic exhumation stages. Thus, we will refrain from placing emphasiz on the significance of active and passive cooling processes and the focus of this paper remains on the geological record of cooling curves of different shape.

2.1 Geologically relevant parameter range

The model for cooling during exhumation discussed above allows to estimate the range of geologically reasonable cool-

ing rates by assuming reasonable ranges of initial geothermal gradients and exhumation rates. The lower limit of g may be given by about 10°C/km which corresponds to a P/T ratio of low temperature metamorphic rocks that reside at 35 km depth and 350 °C at the start of exhumation. An upper limit may be given by the highest possible crustal geotherm that may be reached conductively. This may be attained if the Moho coincides with the lithosphere-asthenosphere boundary (about the 1200 °C isotherm). If this is located at, say, 30 km, then the upper reasonable limit for a linear thermal gradient through the entire lithosphere is given by about 40 °C/km. A reasonable range of exhumation rates may be between hundreds of metres per my and several km/my (BEAUMONT, 1992; ZEITLER, 1985). Using eq(5) of Appendix 2 this parameter range results in cooling rates between about ten and some hundreds of °C/my at 500-600 °C (Fig. A1) which is realistic, given some documented cooling rates (CLIFF et al., 1985).

If cooling is caused by the termination of a contact metamorphic heating process, then the contact metamorphic model discussed above can be used to estimate the magnitude of cooling rates. Cooling curves of rocks that lie within, say, 10 km of an igneous intrusion of size d, may be described in the region ($d/2+10$ km) $>z>$ $d/2$ (Fig. 1). Depending on the size of the heat source between d = 100 m and d = 10 km, cooling rates described by eq(7) range between 1 °C/my and many 1000 °C /my (Fig. A2). The thermal consequences of processes like delamination of the mantle lithosphere in the Earth's crust may also be described as contact metamorphism in the widest sense. This process is followed by cooling and refreezing of the mantle lithosphere and is therefore also a thermal relaxation of an initial temperature perturbation. The process has been previously described by cooling of a semi-infinite half space (MCKENZIE, 1978). The cooling curves described by the present model are very similar in shape to the cooling curves described by MCKENZIE (1978). The major difference being in minor differences in the absolute cooling rates. Therefore, the thermal effects of some tens of kilometres of delaminating and refreezing lithosphere in the middle crust may be described with the intrusion model. Cooling rates of this process as predicted by eq(7) of Appendix 2 are of the order of 1 °C/my. Cooling histories of magmatic bodies are readily described in the region $z<d/2$. Low-P high-T terranes of the granulite facies have been described as regions that have been pervasively heated by advective heat sources. Thus, some low-P high-T terranes may also be described in the region $z<d/2$. At the time of their metamorphic peak, the temperature distribution across a low-P high-T terrane may also be roughly step-shaped and the subsequent cooling history may be described by this model. For most intrusion sizes and $z<d/2$, maximum cooling rates are of the order of some tens to hundreds °C/my (Fig. A1, b).

2.2 Time scales of conductive and advective cooling processes

From above, it may be seen that cooling rates of different cooling processes may be of the same order. Cooling rates of some tens of °C/my are typical for a large range of reasonable exhumation rates and thermal gradients. They are also typical during cooling of igneous intrusions that are larger than about 20 km (Figs. A1, A2). Passive cooling during lithospheric cooling, forming concave cooling curves, is extremely slow, but may be matched by cooling rates during slow exhumation. A comparison of the thermal time constant (a measure of the duration of passive cooling history) with the realistic exhumation rates (a measure of the duration of an active cooling history) confirms these parallels. The thermal time constant of a thermal event expands with the square of its length scale so that:

$$\tau = \frac{L^2}{\kappa} \tag{1}$$

where L is the length scale of the thermally perturbed region, κ is the thermal diffusivity and τ is the thermal time constant (Table 1). Therefore, the thermal time constant, τ, of a ten kilometre sized intrusion is about 3 my, τ of a 35 km thick crust is of the order of 40 my and τ of a 100 km thick lithosphere is of the order of hundreds of my. These values may be compared with the total duration of cooling during exhumation of metamorphic rocks. The three thermal time constants and length scales mentioned above correspond to exhuming these length scales L = 10, 35 and 100 km at rates of U = 3.3 km/my; U = 0.9 km/my and U = 0.3 km/my. Since these numbers are within a reasonable range of denudation rates, cooling rates from cooling due to exhumation and due to thermal relaxation (active and passive cooling) are expected to be of the same order. A direct comparison of the relative importance of different cooling processes may be performed by considering the dimensionless Peclet number, P_e. This number is useful to predict if passive or active cooling processes will dominate the shape of the cooling curve when these processes occur simultaneously. The Peclet number is defined as:

$$P_e = \frac{LU}{\kappa} = \frac{U\tau}{L} \tag{2}$$

For Peclet numbers near one, cooling due to exhumation and cooling due to thermal relaxation are of similar importance. For Peclet numbers much larger than one, cooling due to exhumation will be much more important and – given the restrictions on the exhumation process of the model used here – convex cooling curves may be expected. For Peclet numbers much smaller than one, passive cooling will dominate and concave cooling curves may be expected. The geological parameters discussed above show Peclet numbers near P_e = 1 are possible. This indicates that absolute cooling rates may be similar for a range of cooling processes so that other criteria must be sought to discriminate between them.

3. Geological record of differently-shaped cooling curves

It will now be investigated to what extent the difference in shape between convex and concave cooling curves is recorded in metamorphic rocks. Because of the circular problem of having to assume a cooling rate to derive a cooling rate from different isotopic systems with different closure temperatures, we refrain from discussing the geological record in isotopic systems. Rather, we utilise the record of closure temperatures of a single diffusing system subject to the model cooling curves discussed above. This will now be discussed.

3.1 The diffusion model

In order to investigate the closure temperatures of minerals subject to specified cooling histories we employ the formalism of DODSON (1973, 1986), which relates closure temperature to cooling rate, grain size, diffusion parameters and geometry of the diffusing grain pair. It is given by:

$$s = \frac{D_0}{l^2}\frac{RT_c^2}{Q}e^{\left(-\frac{Q}{RT_c}+G_{(p)}\right)} \tag{3}$$

Table 1
Symbols used in the calculations. *) Diffusion data are those of CYGAN & LASAGA (1985).

SYMBOL	UNITS	EXPLANATION
GENERAL		
T	°C	Temperature
t	s	time
κ	10^{-6} m^{-2} s^{-1}	thermal diffusivity
s	°C s^{-1}	cooling rate
L	m	length scale
τ	s	thermal time constant
PASSIVE COOLING MODEL		
d	m	thickness of one dimensional intrusion
z	m	distance from the centre of the intrusion (z=d/2 is the contact of the intrusion)
T_i	°C	intrusion temperature
T_b	°C	background temperature
t_{Tmax}	s	time of the temperature peak
s_{max}	°C s^{-1}	maximum cooling rate
ACTIVE COOLING MODEL		
U	m s^{-1}	exhumation rate
g	°C m^{-1}	thermal gradient
x	m	distance from the cooling surface
x_i	m	initial depth of rocks
DIFFUSION MODEL		
D_0	9.8 x 10^9 m^2 s^{-1}	pre-exponent diffusion coefficient*)
Q	239 kJ mol^{-1}	activation energy*)
R	8.3 J mol^{-1} K^{-1}	gas constant
$G_{(p)}$	7.12	geometrical parameter for closure of grain centre in spheres
T_c	K	closure temperature
l	m	grain size of slower diffusing mineral grain

All parameters are defined in Table 1. Details of the assumptions and boundary conditions used to formulate eq(3) are not reiterated here and the interested reader is referred to the original contributions of DODSON (1973, 1986) and a number of applications of this formalism (e. g.: EHLERS et al., 1994a, b). The cooling rate derived from eq(3) is the cooling rate at the closure temperature, Tc. Therefore, substantial parts of a cooling curve may be established from mineral pairs that close at different temperatures. This may be given by the closure of different exchange systems, but may also be given by closure of the one ion exchange system in grain pairs of different size (MENGEL & RIVERS, 1991; EHLERS et al., 1994b). Here, we investigate the closure record of different grain sizes for the example of Fe-Mg exchange between garnet and biotite. Using closure temperatures of grains of different known sizes of only one exchange equilibrium has the enormous advantage that the results are not affected by lack of knowledge of the exact diffusion coefficients. This is because the error in knowledge of the diffusion coefficients is a systematic error and will not affect the relative results on the shape of the cooling curve. It is emphasized that we apply eq(3) only to illustrate, qualitatively, how different cooling curves may be recorded. For faster diffusion coefficients than those given in Table 1 cooling rates in a lower closure temperature bracket will be recorded, for slower diffusion coefficients closure will occur at higher T. For a discussion of a statistic elimination of problems arising from estimating grain size in thin section we refer to EHLERS et al. (1994b). Eq(3) was derived for cooling histories that are linear in T^{-1} but it is a good approximation to many other cooling curves (LOVERA et al., 1989). Therefore, T_c can, in

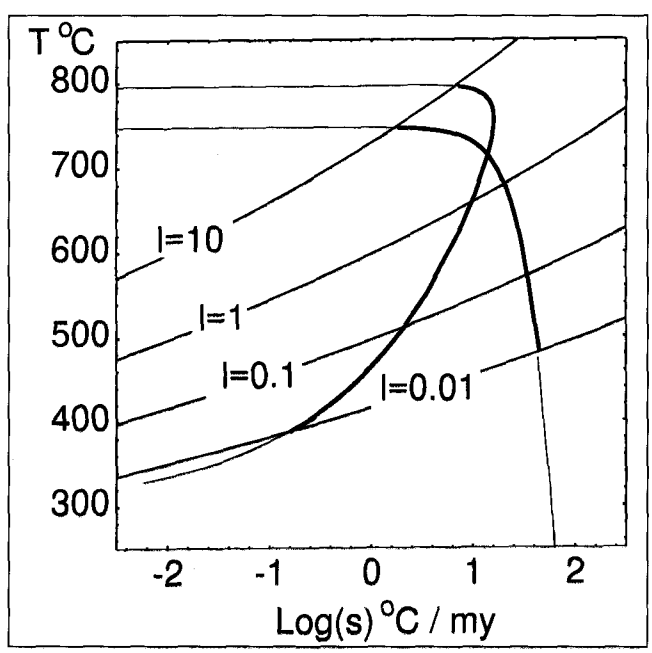

Fig. 3
The closure temperature record of active and passive cooling curves. The diagram is a reproduction of the cooling curves of Fig. 2 superimposed on closure curves calculated with eq(3) and parameters of Table 1. The thick part of the cooling curves are those likely to be recorded by garnet-biotite grain pairs of different grain sizes. The labels are for grain size of garnet in millimetres. Note that closure temperatures of 750 °C are recorded by smaller grains for the concave and by larger grains for the convex curve, while 500 °C are recorded by larger grains for the concave and smaller grains for the convex cooling curve.

principle, be calculated by substitution of any analytical relationship describing a cooling curve into eq(3). This is illustrated in Figure 3 for the examples of a convex and a concave cooling curve from Figure 2. Closure temperature – cooling rate relationships as calculated with eq(3) are shown for four different grain sizes. The intersection of the cooling curves with the closure curves as given by eq(3) may be interpreted as the closure temperatures and closure cooling rates for the specified grain size. It may be seen that the two cooling curves will record similar closure temperatures in grains between 0.01 mm and 10 mm in size. Indeed, grains of about 3 mm size will record an identical T_c = 690 °C and corresponding s = 12 °C/my for both cooling curves. However, at lower temperatures, concave cooling curves will record decreasing cooling rates with decreasing temperature, while convex cooling curves will close in a narrower temperature interval and will record increasing cooling rates with decreasing temperatures. This depends on which part of the cooling curve intersects the closure interval of grain sized that can reasonably be observed. In the following we present calculations to evaluate a large range of cooling curves with this model for closure temperature in order to establish if the shape of such cooling curves can be recorded in the thermometric record.

3.2 Results

A large range of convex and concave cooling curves were evaluated with the model above in order to assess how the curvature of a cooling curve may be recorded. On Fig. 4, these cooling curves are superimposed on the closure interval of garnet-biotite equilibria for a grain size range of garnets between 0.05 mm and 5 mm. This closure interval is shown as the shaded area and the part of each cooling curve that is within this area may be interpreted as the range of closure temperatures and cooling rates recorded in a rock containing garnets of a grain size range which is reasonably observable in thin section. Concave cooling curves are evaluated with our model for passive cooling curves using a range of different z (Fig. 4a), different d (Fig. 4b) and different T_b (Fig. 4c). Convex cooling curves are evaluated with our model for active cooling applying a range of different erosion rates, U, (Fig. 4d) and different initial depths, x_i, (Fig. 4e). It may be seen that a significant part of most cooling curves will be recorded thermometrically by a grain size range that commonly is present in garnet and biotite bearing rocks. As all cooling curves must commence with an initial increase of cooling rate following the metamorphic temperature peak (where the cooling rate is zero), both passive and active cooling curves record a negative T_c-s relationship at high temperatures. Passive cooling curves may record this if the metamorphic peak temperature is within or near the closure interval. However, during continued cooling, passive cooling curves will record a distinctly concave part of the cooling curve. For all passive cooling curves cooling rates are much slower at the low-temperature end of the closure interval than at higher temperatures. For example, the cooling curves explored for different intrusion sizes d (Fig. 4b) record usually about one order of magnitude slower cooling rates in 0.05mm grains (closing at 400 °C – 600 °C depending on d) than in 5mm sized grains (closing at 700 °C – 800 °C). The recorded part of the concavity increases if the background temperature is higher (Fig. 4c). Then, cooling rates will approach zero at temperatures that are still within the closure interval. The cooling curve for T_b = 500 °C records 3-4 orders of magnitude of cooling rates in the clo-sure range between 500 °C and 700 °C as is evidenced by a large grain size range recording these temperatures. In convex cooling curves, on the other hand, the relationship between closure temperature and cooling rate is inverse to pas-sive cooling curves and the garnet-biotite equilibrium may record a much smaller range of closure temperatures for the same grain size range. The difference between fast cooling rates recorded at low T and slow cooling rates recorded at high T is not as large as it is for the passive cooling curves. However, depending on the transport rate, it still may be about one order of magnitude.

4. Discussion with examples

The results of the last section have shown that the difference in shape between convex and concave cooling curves – at least for the simplistic models chosen here – may be recorded in metamorphic rocks via their contrasting closure temperature – grain size relationships. Clearly, cooling curves caused by natural cooling processes may not always be strictly convex or concave and may deviate substantially from the simple shapes of the model examples used here. Different cooling processes in nature may therefore not be easily distinguished from established convex or concave cooling curves. For example, if exhumation of rocks occurs not at a constant rate U, but decreases with time, then the low temperature part of the active cooling curves shown in Fig. 1b, 2, 3, 4d,e may become concave towards the time axis at very low temperatures. Correspondingly, passive cooling histories that commence at peak temperatures within the closure interval of Fig. 4 must record an initial increase of the cooling rate with decreasing temperature. These are but two examples where an interpretation of the shape of the cooling curve may be misleading. Moreover, active and passive cooling processes may compete, resulting in complicated cooling curves with more than one sense of curvature. For example, when magmas intrude into rocks that cool during exhumation, as may be the case during continental extension, then active cooling processes may be superimposed by passive cooling processes. Regardless of these possible complications, many cooling curves published in the literature have comparably simple shapes and both, convex and concave cooling curves have been documented (Fig. 5). It is not the purpose of this discussion to evaluate all possible geological interpretations of the curvature of such published cooling curves. Rather, we focus simply on determining if the curvature of cooling curves established in the literature may also be recorded in the closure record of garnet-biotite equilibria. If this is so, then this may be used to place an independent constraint on geochronologically determined cooling curves. Thus, we begin with the discussion of some simple cooling curves with well-

Fig. 4 →
The evidence of active and passive cooling curves in metamorphic rocks as recorded by the closure temperature in garnet biotite equilibria of a range of grain sizes. The closure interval is shown as the shaded area which is bound by the closure curve for 5mm sized grains at the high T end and 0.05 mm sized grain pairs at the low T end. Figs. 4a, b and c are for passive cooling curves, Figs. 4d, e are for active cooling curves. Fig. 4a is for d = 60 km, T_i = 800 °C, T_b = 300 °C and five different z labeled in kilometres. Fig. 4b is for z = 0 and five different intrusion sizes labeled in kilometres. Fig. 4c is for d = 10 km, z = 0 and for three different T_b labeled in °C. Fig. 4d shows active cooling curves with g = 30 °C/km and x_i = 25 km for five different exhumation rates labeled in km/my. Fig. 4e shows active cooling curves for x_i = 25 km, U = 1 km/my and five different initial thermal gradients labeled in °C/km.

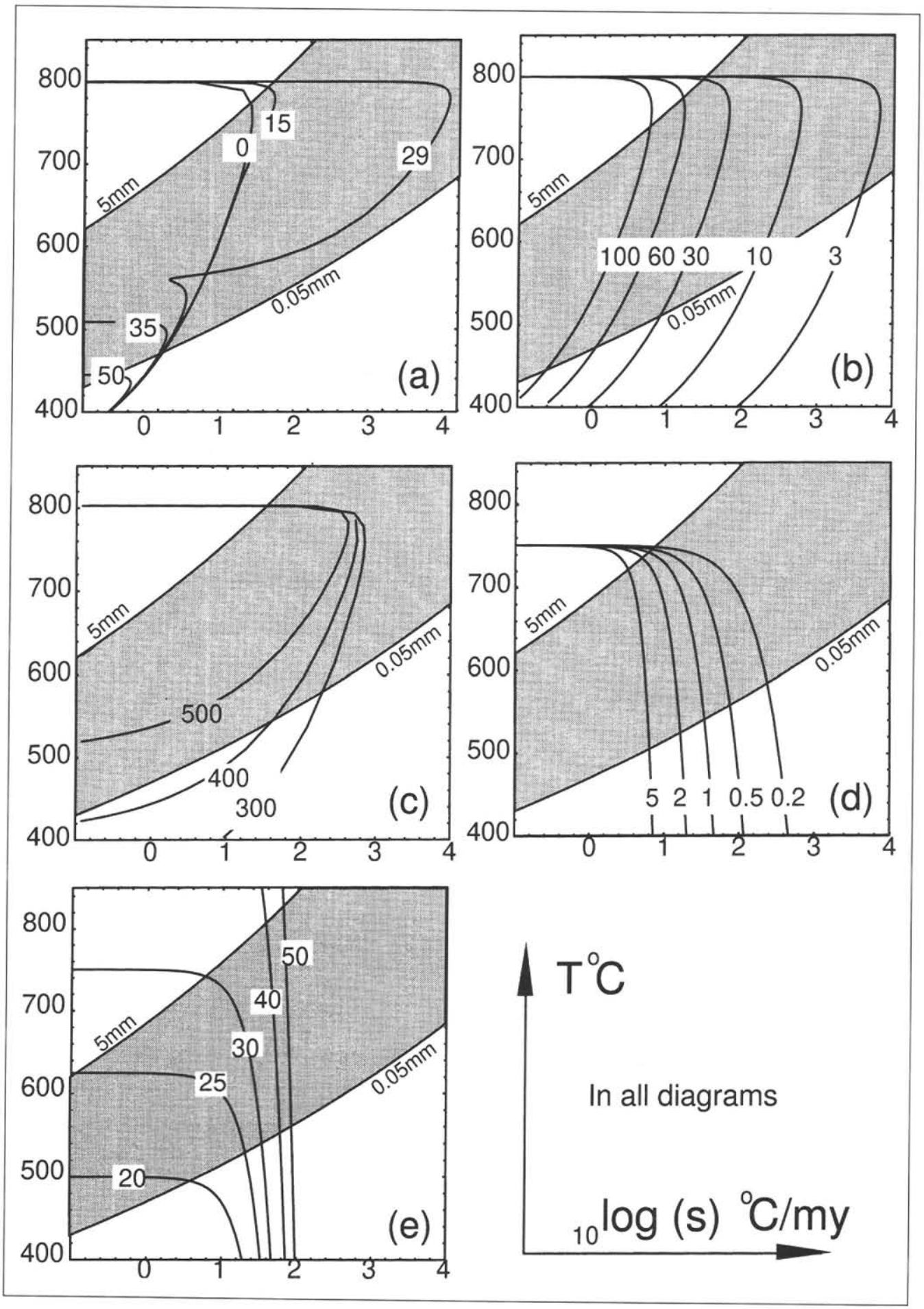
800
700
600
500
400
0 1 2 3 4
5mm
0.05mm
0
15
29
35
50
(a)
100 60 30
10
3
(b)
500
400
300
(c)
5 2 1 0.5 0.2
(d)
50
40
30
25
20
(e)
T°C
In all diagrams
10log (s) °C/my

defined cooling causes. In all examples discussed below, cooling curves (Figs. 5a,c,e) were fitted to data from the literature using best fit polynomiam expressions which were fitted to the data with the computer software MATHEMATICA. The corresponding cooling rate evolutions shown in Figs. 5b,d,f are found by differentiation of the polynomial expression. The cooling curves – established by numerical fitting of geochronological data – will serve us as the starting assumption. It is emphasised that the data as well as the cooling curves inferred from them have been subject to some debate. However, it is not the purpose of the present paper to discuss the validity of these curves. Rather, we assume the data and curves to be correct and focus on the prediction of these curves for the geothermometric record of the parageneses.

4.1 The Quottoon pluton and Glen Dessary syenite

Fig. 5a shows cooling histories of two igneous intrusions, the Quottoon pluton in British Columbia (HARRISON et al.,1979) and the Glen Dessary syenite (VAN BREEMEN et al., 1979; CLIFF, 1985). As is to be expected for cooling of igneous rocks, the cooling curves for both bodies are strictly concave indicating thermal relaxation and asymptotic equilibration of the temperatures to the ambient state. In the two examples shown, the transition from rapid cooling to slow cooling occurs at very low temperatures, below, say, 300 °C. As a consequence, the cooling rate curves shown on Fig. 5b are very steep inside the closure interval (shaded areas) and track to lower cooling rates only below the closure interval. Vertical lines on the cooling rate figures means constant cooling rate throughout the thermal evolution. This is a linear temperature-time curve which is difficult to interpret. Nevertheless, the two cooling curves cover a difference in cooling rate at the high and low temperature end of the closure interval which is near half an order of magnitude. This shape is characteristic of their passive cooling history. Therefore, if slower cooling rates can be documented in smaller grain sizes, then this is a good indicator of a concave cooling curve.

4.2 Central Swiss Alps

Fig. 5c shows two sets of radiometrically determined age data from the central Swiss Alps (VANCE & O'NIONS,1992). They are from the Steinetal and the Bellinzona regions. VANCE and O'NIONS (1992) interpreted cooling curves of different shapes from these data for these two regions, in particular a convex cooling curve for the Steinetal and a concave cooling curve for the Bellinzona region. Fig. 5d shows that – if these cooling curves are correct – this difference in shape is indeed likely to be recorded by garnet – biotite equilibria. In particular, the Steinetal evolution shows an increase of cooling rate over about one order of magnitude, as recorded by a range of closure temperatures between 450 °C and 500 °C in grains between 0.01 and 0.05 mm in size. The Bellinzona rocks show slowly decreasing cooling rates for lower closure temperatures as documented by a much larger range of closure temperatures in the same grain size range. The shape difference of these two cooling curves has been interpreted as the consequence of erosion-versus extension-driven exhumation (VANCE & O'NIONS, 1992). However, it is noted that the samples were taken from a large area which also includes the Simplon line. Details of the cooling history and causes for cooling have been discussed by GRASEMANN & MANCKTELOW (1993) and references therein.

4.3 The Glein and Koralm region

The two example from the eastern Alps shown in Fig. 5e,f illustrate this further. A cooling curve for the Gleinalm complex has recently been documented in the temperature range between 500 °C and 100 °C (NEUBAUER et al., 1995). It has been fitted by a slightly concave cooling curve, but the data indicate that the cooling curve is probably approximately linear (Fig. 5c). Especially in the temperature range of interest, above say 300 °C. The curvature of the cooling curve is minimal (Fig. 5e). This is reflected by the predicted grain size – closure temperature relationships. Fig. 5f shows that garnets in the Gleinalm region are predicted to record 400-500 °C in the grain size range between 0.01 mm and 0.05 mm which corresponds to a largely constant cooling rate in this temperature interval. Detailed correlation of the absolute ages of this cooling curve with sedimentological data from adjacent basins and structural data showed that this cooling curve is likely to be the consequence of exhumation (NEUBAUER ET al., 1995). However, in an adjacent area to the south, the Koralm, an extremely concave cooling curve has been established for a large shear zone in the region, the Plattengneiss, on the basis of garnet-biotite thermometry (Fig. 5e) (EHLERS et al., 1994). The cooling curve is comparable to the cooling curve of the center of a 10 km wide one-dimensional step-shaped temperature distribution and it is more difficult to explain with cooling due to exhumation. The two cooling curves cannot be directly compared because they were derived for different geographical regions. However, it is suggested that the temperature ranges over which they have been documented complement each other. It is suggested that the high temperature part of both cooling histories is unrelated to depth changes of the rocks. Rather it may be related to passive cooling from an independent heating process, for example shear heating.

5. Conclusion

(1) Cooling curves of metamorphic rocks may be classified in convex and concave cooling curves. The former are convex

Fig. 5 →
A number of convex and concave cooling curves from the literature and their corresponding cooling rate evolutions. Cooling curves are fitted with polynomial fits in MATHEMATICA for radiometric age data from the literature (black dots). Cooling rate evolutions are superimposed on the closure interval for garnet-biotite equilibria for garnet grains between 5 mm and 50 μ (dark shaded region) and between 50 μ and 10 μ (light shaded region). Thick parts of the cooling rate curves are those likely to be recorded in metamorphic rocks. (a) Shows the cooling curves of VANCE & O'NIONS (1992) for part of the central Swiss Alps. Their data are fitted with the relationship T = (503.069sin(t/17)-1.02) for the Steinetal and by T = (0.9029 t^2 - 38.962) for the Bellinzona region. T in these relationships is in my. (c) shows the cooling curves for the Gleinalm (NEUBAUER et al., 1995) and for the Koralm (EHLERS et al., 1994a), both in the Austroalpine of the eastern Alps. The Gleinalm cooling data are fitted with the relationship T = (41.331+26.783 x 1.03^t) , the Koralm cooling curve is that given by the relationship of EHLERS et al (1994a): T = (ln(0.0355 t)-27.2)/0.0355 - 273. (e) Two cooling curves for two igneous rocks, that of the Quottoon pluton in British Columbia (HARRISON et al., 1979) and that of the Glen Dessary syenite in Scotland (VAN BREEMEN et al., 1979; CLIFF, 1985). These two curves are fitted by T = (101.907+2.09854 10 -51.4^t + 0.4717^t) for the Quottoon pluton and by T = (64.41 + 0.514 1.03^t) for the Glen Dessary syenite. (b), (d) and (f) show the corresponding cooling rate evolutions as found by differentiation of the polynomial fits.

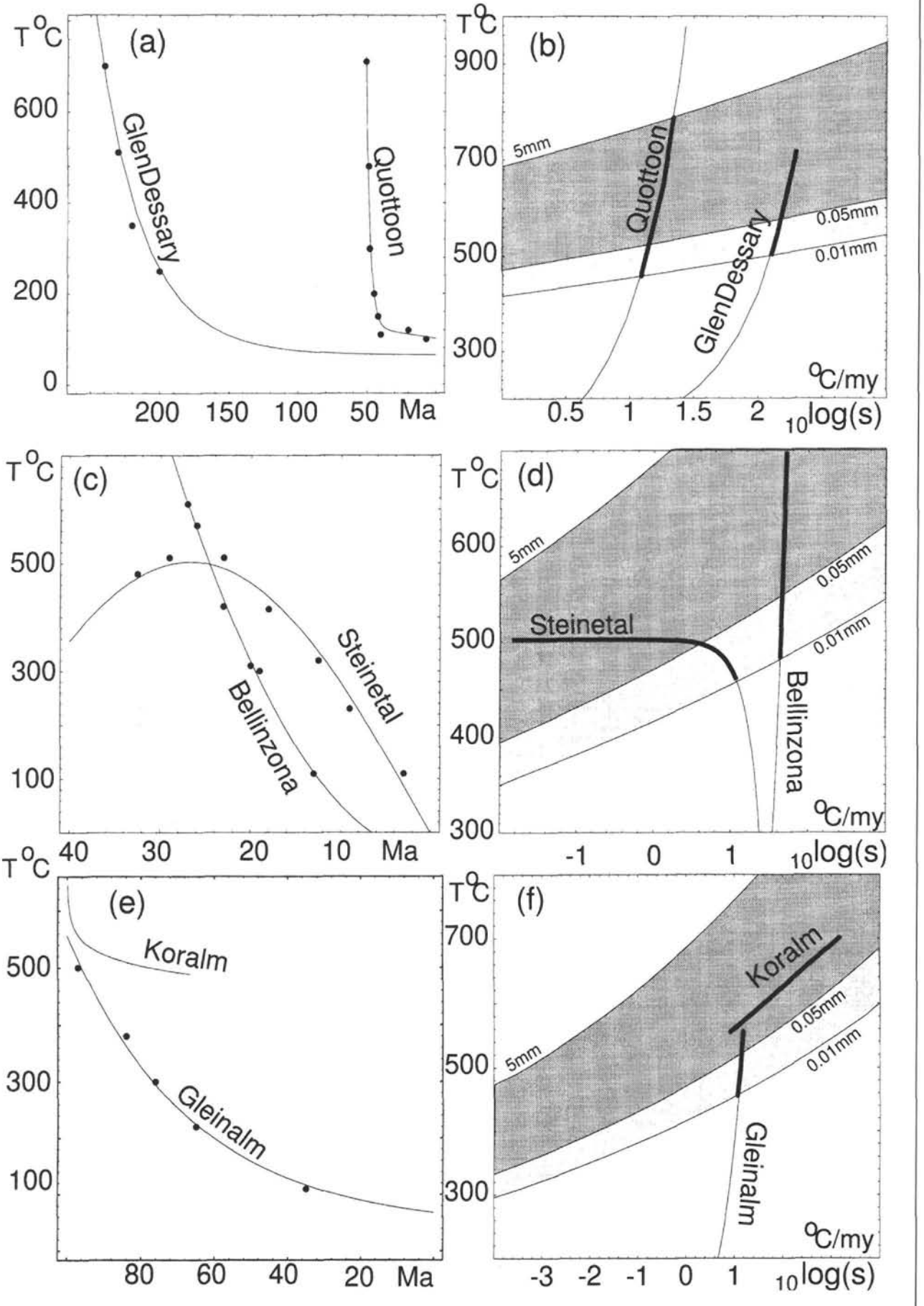
(a)
T °C
600
400
200
0
GlenDessary
Quottoon
200 150 100 50 Ma
(b)
T °C
900
700
500
300
5mm
0.05mm
0.01mm
Quottoon
GlenDessary
°C/my
0.5 1 1.5 2 10log(s)
(c)
T °C
500
300
100
Steinetal
Bellinzona
40 30 20 10 Ma
(d)
T °C
600
500
400
300
5mm
0.05mm
0.01mm
Steinetal
Bellinzona
°C/my
-1 0 1 10log(s)
(e)
T °C
500
300
100
Koralm
Gleinalm
80 60 40 20 Ma
(f)
T °C
700
500
300
5mm
0.05mm
0.01mm
Koralm
Gleinalm
°C/my
-3 -2 -1 0 1 10log(s)

upwards in a temperature-time diagram and have a negative slope in a temperature-cooling rate diagram. The latter are concave upwards in a temperature-time diagram and have a positive slope in a temperature-cooling rate diagram. Convex cooling curves may produced by exhumation of rocks at a constant rate. We term this process *active* cooling. Concave cooling curves may be caused by thermal relaxation at the end of a heating process, for example cooling of igneous intrusions or contact metamorphism. We term this process *passive* cooling. However, care must be taken in inferring a cooling cause from the shape of a cooling curve as both active and passive cooling can produce cooling curves of all shapes, depending on the boundary conditions of the cooling process.

(2) Concave and convex cooling curves may be recorded by closure temperatures of geothermometric systems. For concave cooling curves, grains of a large range of grain sizes will record similar closure temperatues. For convex cooling curves, there will be a large spread in closure temperatures with a strong grain size dependence. Geothermometrically derived closure temperature – cooling rate relationships bear therefore important information on the shape of cooling curves and potentially information on the cooling process. This places an independent constraint on geochronologically determined cooling curves. Such an independent constraint is extremely valuable as it is free from the problems of uncertain closure temperatures at different cooling rates. Moreover, it is possible that cooling curves can be documented in more detail than can be documented by geochronological means, as a much wider range of clodure temperatures may be available, given the appropriate grain size range.

(3) Application of the model to cooling curves from the central Swiss Alps and the Glein-Koralm region in the Eastern Alps predicts that garnet-biotite equilibria in differently-size grain pairs may record characteristic closure temperature – grain size relationships from which the curvature of the cooling curve can be interpreted. For example, closure temperatures of garnets are predicted to vary as a function of grain size in the closure interval for the Bellinzona region, but vary little with grain size in the Steinetal region. In the eastern Alps, closure temperatures of garnet biotite equilibria are predicted to vary more strongly with grain size in the Gleinalm region than in the Koralm region. However, it is emphasized that these predictions rely on the veracity of previously published cooling curves.

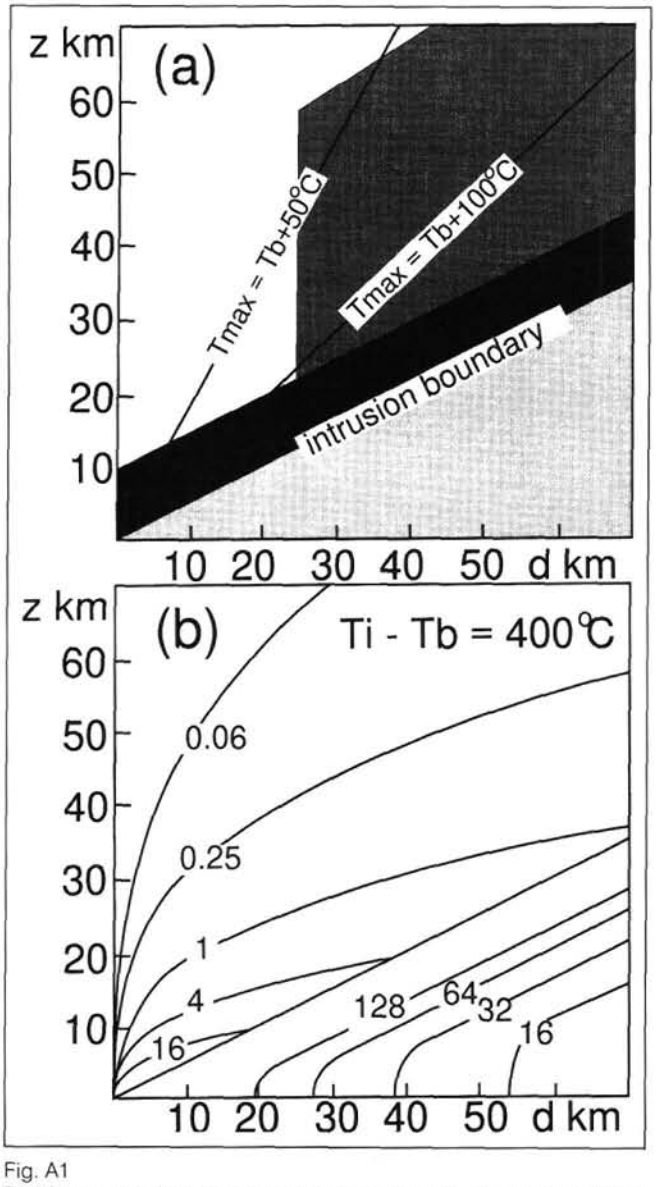

Fig. A1
Passive cooling histories parameterised in terms of diameter d (km) of an intrusion and distance z (km) from its center. Note that, from the definition of d and z all $|z| < d/2$ are inside the intrusion. Fig. A2a shows how different regions of this parameter space may be used to describe different forms of metamorphism. The light shaded region is inside the thermal perturbation. It can be used to describe the cooling history of igneous rocks and may be appropriate to describe many regional low-P high-T terrains. The black region may be appropriate to describe contact metamorphism around igneous intrusions. The dark shaded region may be used to describe thermal effects in the crust as the consequence of delamination and conductive refreezing processes of some tens of kilometres of the sub-crustal mantle lithosphere. Figs. A2b shows the maximum cooling rate s_{max} for $\Delta T = T_i - T_b = 400$ °C.

Appendix 1

Here, a geologically relevant range of absolute cooling rates that may occur during cooling due to exhumation and cooling following contact metamorphism are calculated using the models for active and passive cooling discussed int he text. Cooling rates for a large range of cooling curves during passive cooling may conveniently be shown for a given ΔT, ($\Delta T = T_i - T_b$) in a diagram plotting z versus d and contouring for maximum cooling rate s_{max} (Fig. A1). From the definition of z and d (Table 1) all $|z| < d/2$ are within the intrusion and may thus describe cooling curves of dikes and sills, while all $|z| > d/2$ are outside the intrusion and may describe various forms of contact metamorphism. The shaded regions on Fig. A1a show different forms of metamorphism that may be described in this diagram. Fig. A1b shows s_{max} for $\Delta T = 400$ °C. For all forms of contact metamorphism outside large intrusions, cooling rates are substantially smaller than 10 °C/my. Only for intrusion sizes smaller than 10 km cooling rates are larger. For larger ΔT cooling rates increase. At $\Delta T = 1000$ °C cooling rates are about twice as rapid as those shown in Fig. A1b. Cooling rates are higher inside the intrusion. They approach infinity at the inside of the contact and decrease towards the center. Depending on ΔT, maximum cooling rates are of the order of several tens of °C/my for all thicknesses of 50 km or less and at least 100 °C/my for all intrusion thicknesses of 20 km thickness or less. For the ΔT shown here, cooling rates exceed 1000 °C/my inside the intrusion within about 3-5 km of the contact.

A large range of cooling rates for cooling due to exhumation, resulting convex cooling curves, may be shown in a

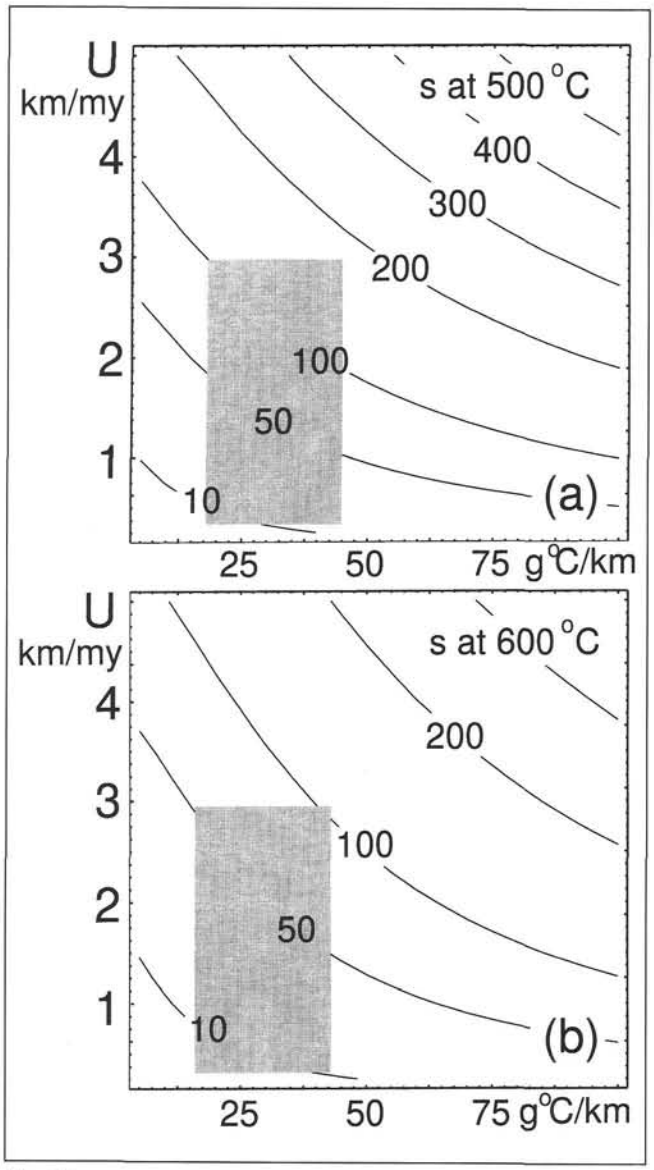

Fig. A2
Active cooling histories parameterised in terms of the exhumation rate U in km/my and a linear thermal gradient g in °C/km. The diagram is contoured for s in °C/my at 500 °C (Fig. A1a) and 600 °C (Fig. A1b). The diagram is drawn for rocks with a peak temperature T_{max} = 700 °C. Different cooling rates on this diagram are therefore for rocks originating from depths corresponding to x_i = 700 °C/g along the thermal gradient axis. The shaded area indicates a geologically likely region of the parameter space.

diagram of U versus g, contoured for cooling rate at a given temperature. Fig. A2 shows the cooling rates at 500 °C and 600 °C of rocks with a T_{max} of 700 °C. Cooling rates are shown at such high T because these are likely to be recorded by the parageneses. Cooling rates at lower T are more rapid. For any given temperature, cooling rates are fastest for large thermal gradients, g, and large velocities U. The cooling rates are somewhat higher at 500 °C than at 600 °C but, in particular for low U and g, the differences are small. For U between 500 m/my and 5 km/my and thermal gradients around 20 °C/km, cooling rates vary between 10 °C/my and about 150 °C/my. At thermal gradients of 40 °C/km, cooling rates vary between 12 °C/my and 300 °C/my for the same range of U. Note that the cooling rates also depend on the peak temperature prior to the onset of relative motion, which is coupled with initial distance of a rock from the cooling surface through the thermal gradient. Lower peak temperatures imply closer distance for the same gradient. Therefore, cooling rates at a given temperature will be higher for lower peak temperatures and lower for higher peak temperatures.

Appendix 2

The simple models describing concave and convex cooling curves used in this paper are based on analytical solutions of the one-dimensional heat flow equation:

$$\frac{dT}{dt} = \kappa \frac{d^2T}{dx^2} \tag{4}$$

In this equation, T is temperature, t is time, κ is the thermal diffusivity and x is a spatial variable. When describing concave cooling curves, z is used instead of x as the spatial variable in order to discriminate between different descriptions. The different solutions of this equation discussed below arise from the different boundary and initial conditions used to describe convex and concave cooling curves.

Convex cooling curves are described with a simple model for cooling due to exhumation. The assumed initial temperature condition is given by a one-dimensional column with a linear thermal gradient: $T = gx$. After $t = 0$ it is assumed that this column moves at constant velocity U towards a surface of constant temperature $T = 0$ at $x = 0$. At $x = \infty$ it is assumed that the temperature remains constant. An analytical solution of the heat flow equation for these boundary and initial conditions is given by CARSLAW & JAEGER (1959) :

$$T_t = gx - gUt + \frac{g}{2}\left((x+Ut)\mathrm{e}^{Ux/\kappa}\mathrm{erfc}\left(\frac{x+Ut}{\sqrt{4\kappa t}}\right) + (Ut-x)\mathrm{erfc}\left(\frac{x-Ut}{\sqrt{4\kappa t}}\right)\right) \tag{5}$$

In eq(5), U and g are interpreted as the exhumation rate and the geothermal gradient, respectively. In eq(5), $x = (x_i - U\,t)$ where x is the depth of a rock as a function of time and x_i is its initial depth. Eq(5) describes cooling curves that are strictly convex upwards in T-t space.

Concave cooling curves are described with a simple model for passive cooling. The thermal relaxation history of an initial, one-dimensional, step-shaped temperature distribution is used. For this, the thermal evolution may be formulated in terms of the thickness of the temperature perturbation, d, and the distance from its center, z:

$$T = T_b + 0.5(T_i - T_b)\left(\mathrm{erf}\left(\frac{0.5d-z}{\sqrt{4\kappa t}}\right) + \mathrm{erf}\left(\frac{0.5d+z}{\sqrt{4\kappa t}}\right)\right) \tag{6}$$

(e. g.: CARSLAW & JAEGER, 1959) (see Table 1 for explanation of parameters). The cooling rate evolution is described by:

$$s = \frac{dT}{dt} = \frac{(T_i - T_b)}{4t\sqrt{\pi\kappa t}}\left(\frac{z-0.5d}{\mathrm{e}^{((0.5d-z)^2/4\kappa t)}} - \frac{z+0.5d}{\mathrm{e}^{((0.5d+z)^2/4\kappa t)}}\right) \tag{7}$$

The time of the metamorphic temperature peak, t_{Tmax}, is found by setting eq(7) to zero (because $s|_{t\,=\,Tmax} = 0$) and solving for T:

$$t_{T_{\max}} = -\frac{zd}{2\kappa \ln\left(\frac{z-0.5d}{z+0.5d}\right)}. \tag{8}$$

The metamorphic peak temperature, T_{max}, is calculated by substituting eq(8) into eq(6). The time of the maximum cooling

rate, $t_{s\,max}$ can be found by differentiating eq(7) with respect to time and setting the result to zero:

$$e^{\left(\frac{dz}{2\kappa t}\right)} = \left(\frac{6(0.5d - z)\kappa t - (0.5d - z)^3}{6(0.5d + z)\kappa t - (0.5d + z)^3}\right). \quad (9)$$

From that, the maximum cooling rate, s_{max}, may be found by solving eq(9) iteratively for time and substituting that into eq(7). Depending on z, these relationships describe temperature-time curves that are concave towards the time axis.

Acknowledgements

N MANCKTELOW, B GRASEMANN, F NEUBAUER and W FRANK are thanked for a series of discussions on the thermal evolution of the Simplon region and the Glein-Koralm region, respectively. T RIVERS, R JAMIESON, M WILLIAMS and K HODGES are thanked for a number of discussions and constructive comments in an earlier version of this manuscript. B GRASEMANN and an anonymous reviewer are thanked for their review and their reminders to place some more question marks around our interpretation of cooling causes from cooling curves. The research of this paper was supported by the Australian Research Council. The manuscript was finalised as part of FwF project P-12846-GEO.

References

BEAUMONT, C., FULLSACK, P. & HAMILTON, J., 1992: Erosion control of active compressional orogens, in: Thrust tectonics edited by McClay K.R., pp.1-19.

VAN BREEMEN, O., AFTALION, M., PANKHURST, R. J. & RICHARDSON, S. W., 1979: Age of the Glen Dessary syenite, Invernessshire: diachronous Paleozoic metamorphism across the Great Glen. Scottish Journal of Geology, 15: 49-62.

CARSLAW, H. S. & JAEGER, J. C., 1959: Conduction of Heat in Solids, 510pp., Oxford University Press, Oxford.

CLIFF, R. A., 1985: Isotopic dating in metamorphic belts. Journal of the Geological Society London, 14, 97-110.

CLIFF, R. A., DROOP, G. R. T. & REX, D. C., 1985: Alpine metamorphism in the southeast Tauern window, Austria, 2. Rates of heating cooling and uplift. Journal of Metamorphic Geology, 3: 403-415.

CYGAN, R.T. & LASAGA, A.C., 1985: Self-diffusion of magnesium in garnet at 750 to 900 °C. American Journal of Science, 285: 328-350.

DODSON, M. H., 1973: Closure temperature in cooling geochronological and petrological systems. Contributions to Mineralogy and Petrology, 40, 259-274.

DODSON, M. H., 1986: Closure profiles in cooling systems. Material Science Forum, 7,145-154.

EHLERS, K., STÜWE, K., POWELL, R., SANDIFORD, M. & FRANK, W. 1994a: Thermometrically-inferred cooling rates from the Plattengneis, Koralm Region – Eastern Alps. Earth and Planetary Science Letters, 125, 307-321.

EHLERS, K., POWELL, R. & STÜWE, K., 1994b: The determination of cooling histories from garnet-biotite equilibrium. American Mineralogist, 79, 737-744.

ENGLAND, P. C. & THOMPSON A. B.,1984: Pressure-temperature-time paths of regional metamorphism I. Heat transfer during the evolution of regions of thickened continental crust. Journal of Petrology, 25, 894-928.

GRASEMANN, B. & MANCKTELOW, N. S., 1993: Two-dimensional thermal modeling of normal faulting: the Simplon Fault Zone, Central Alps, Switzerland. Tectonophysics, 225, 155-165.

HARRISON, T. M. & CLARK, G. K., 1979: A model of the thermal effects of igneous intrusion and uplift as applied to Quottoon pluton, British Columbia. Canadian Journal of Earth Science, 16, 410-420.

HARRISON, T. M., ARMSTRONG, R. L., NAESER, C. W. & HARAKAL, J. E., 1979: Geochronology and thermal history of the Coast Plutonic complex, near Prince Rupert, British Columbia. Canadian Journal of Earth Science, 16, 400-410.

HODGES, K. V., HAMES, W. E. & BOWRING, S. A., 1994: 40Ar/39Ar ages in micas from a high-temperature low-pressure metamorphic terrain:Evidence for very slow cooling and implications for the interpretation of age spectra. Geology, 22, 55-58.

HOLM, D. K. & DOKKA, R. K., 1993: Interpretation and tectonic implication of cooling histories: an example from the Black Mountains, Death Valley extended terrane, California. Earth and Planetary Science Letters, 116, 63-80.

JAEGER, J. C., 1964: Thermal effects of intrusions. Reviews in Geophysics 2, 443-466.

LOVERA O. M., RICHTER F. M. & HARRISON T. M., 1989: The 40Ar/39Ar thermochronometer for slowly cooled samples having a distribution of diffusion domain sizes. Journal of Geophysical Research, 94, 17917-17935.

LUX D. R., DE YOREO, J. J., GUIDOTTI, C. V. & DECKER E. R., 1986: Role of plutonism in low pressure metamorphic belt formation. Nature, 323, 794-796.

MCKENZIE, D., 1978: Some remarks on the development of sedimentary basins. Earth and Planetary Science Letters, 40, 25-32.

MENGEL, F. & RIVERS, T., 1991: Decompression reactions and P-T conditions in high-grade rocks, northern Labrador: P-T-t paths from individual samples and implications for early Proterozoic tectonic evolution. Journal of Petrology, 32, 139-167.

NEUBAUER, F., DALLMEYER, R. D., DUNKL, I., & SCHRINK, D., 1995: Late Cretaceous exhumation of the metamorphic gleinalm dome, eastern Alps: kinematics, cooling history and sedimentary response in a sinistral wrench corridor. Tectonophysics, 242, 79-99.

SANDIFORD, M., MARTIN, N., ZHOU, S., & FRASER, G., 1991: Mechanical consequences of granite emplacement during high-T, low-P metamorphism and the origin of "anticlockwise" PT paths. Earth and Planetary Science Letters, 107, 164-172.

STÜWE, K., WHITE L., & BROWN R., 1994: The influence of eroding topography on steady state isotherms. Application to Fission Track Analysis. Earth and Planetary Science Letters, 124, 63-74.

STÜWE, K., SANDIFORD, M. & POWELL, R., 1993: On the origin of repeated metamorphic-deformation events in low-P High-T terrains. Geology, 21, 829-832.

VANCE, D. & O'NIONS, R. K., 1992: Prograde and retrograde thermal histories from the central Swiss Alps. Earth and Planetary Science Letters, 114, 113-129.

ZEITLER, P., 1985: Cooling history of the NW Himalaya, Pakistan. Tectonics, 4, 127-151.

Manuskript eingegangen am: 15. 03. 1996 ●
Revidierte Fassung eingegangen am: 15. 09. 1998 ●
Manuskript akzeptiert am: 29. 10. 1998 ●